

Corrosion Characteristics of 304 Stainless Steel in Sodium Chloride and Sulfuric Acid Solutions

Aliaa Abdelfatah¹, A. M. Raslan², Lamiaa Z. Mohamed^{*1}

¹ Mining, Petroleum and Metallurgical Engineering Department, Faculty of Engineering, Cairo University, Egypt

² Materials Division, Metallurgy Department, Nuclear Research Center, Atomic Energy Authority, Cairo, Egypt

*E-mail: lamylomy@yahoo.com, lamiaa.zaky@cu.edu.eg

Received: 14 December 2021 / Accepted: 20 January 2022 / Published: 4 March 2022

Corrosion behavior of austenitic stainless steel 304 (SS) in various concentrations of H₂SO₄ and NaCl solutions was investigated using chemical and electrochemical techniques. Corrosion rate was measured by weight-loss and potentiodynamic polarization. The effects of acid concentrations and voltage scan rate were studied by cyclic voltammetry. Corrosion rate of 304 SS decreases with increasing NaCl concentrations. On the other hand, corrosion rate increasing with increasing the H₂SO₄ concentrations. The surface morphology was characterized by SEM. The elemental analysis was examined by EDX and the elemental distribution by mapping of the corroded 304 SS in different media.

Keywords: Corrosion; 304 Stainless steel; Sodium chloride; Sulfuric acid

1. INTRODUCTION

Stainless steels (SS) are commonly utilized in numerous scientific and engineering applications due to their strong corrosion resistance [1-3]. Corrosion resistance resulted from the creation of a passive film on the SS surface in aqueous media, which protects them from corrosion. For advantages like; thin, extremely adherent, self-repairing, high stability and durability, this passive film is ideal for a variety of applications. At the metal/film interface, the outer layer includes Fe and Cr oxy-hydroxide and hydroxide compounds, whereas the inner layer contains Cr₂O₃ [4, 5]. Although passivation lowers the anodic reaction involved in corrosion, pitting corrosion can still occur in acidic media [3]. Pitting corrosion is frequently undetected until catastrophic damage has occurred as a result of formation of extremely small pit cavity on SS surface, which are always covered by process fluids or heavy layers of corrosion products. Pitting corrosion increased the corrosion rate, which was influenced by pH [6], flow velocity [7], and temperature [8], surface roughness [9], and Cl-ion concentration [1]. As a result, corrosion

control is challenging. Because of the failure of some of SS due to pitting, significant work was devoted to understand and explain pitting behavior, as well as corrosion of numerous SS/environment combinations was investigated [5, 10]. For many industrial applications, they focused on localized corrosion of SS in chloride, chloride/thiosulphate, chloride/sulphide, bromide and bromide/sulphide media [11- 13]. Pitting corrosion is a special form of anodic reaction that results in stimulating and inhibiting to the pit's continued activity [14].

Chloride- and sulfide-ion concentrations influence the passivity breakdown on metal surfaces. These ions diffuse from the film/solution interface to the metal/film interface. When aggressive ions are present in low concentrations, they do not interfere with the metal passivity mechanism; nevertheless, when aggressive anions are present in high concentrations, the potential starts to oscillate because of devastation of passivity by attacker anions. The aggressive anions adsorb to metal ions and promote chemical dissolution; more attacker anions trigger the devastation of the passive layer, resulting in pit formation. The results of cyclic potentiodynamic polarization are utilized to identify the breakdown of passivity and the start of pits on metal surfaces. All chlorides become harmful in the presence of oxygen or hydrogen peroxide [2]. The partial dissolution of sulfide-ion inclusions may result in the formation of pits, which are responsible for pit mouth decoration and, eventually, collapse [15, 16, 17]. The kinetics of passivity and passivity destruction on a SS surface due to hostile anions and pH are studied using potentiostatic measurements. Dastgerdi et al [18] studied the effect of Cl⁻ and pH on the pitting corrosion of 304L SS.

This research aims to study the pitting corrosion resistance of 304 SS in different concentrations of NaCl and H₂SO₄ solutions by weight-loss, potentiodynamic measurement and cyclic voltammetry. The corroded surfaces in different media were characterized by SEM, EDX and mapping for elemental distribution.

2. EXPERIMENTAL WORK

The 304 SS chemical analysis is 0.07%C, 0.62%Si, 0.12%V, 0.21%Co, 0.95%Mn, 17.9%Cr, 0.08%Mo, 7.6%Ni and the rest is iron. The samples were cut with dimension of 1cm x 2cm and thickness 4mm. The 304 SS specimens were tested against corrosion using polarization test with surface area of 0.5 cm². Working electrode was prepared for metallography by using various grades of SiC paper from 100 to 1000 grit, polished by using 0.3 μm alumina paste, polished to 1μm by diamond paste, finally dried using acetone before chemical and electrochemical analysis.

2.1 Weight-loss

All specimens immersed at the same time in the experimental media of NaCl and H₂SO₄ at concentrations of 0.5M and 1M. The weight-loss values of 304 SS were measured after 7, 14 and 21 days intervals from each of these acids. Then, they chemically cleaned to remove the corrosion products.

Using ethanol and distilled water for rinsing the samples then dried and weight measured. All reading taken to be nearest to 0.001g.

The corrosion rate (CR) of specimens were calculated according to Eq. 1 [19]

$$\text{CR (mm/Yr)} = 87.6 \times (\text{W/DAT}) \quad (1)$$

Where W is the loss in weight in milligrams, D is the density in g/cm^3 , A is the area in cm^2 , T is the time of exposure in hours.

2.2 Potentiodynamic Polarization

The electrochemical study performed at 25 °C with PGZ 100 Potentiostat unit including corrosion cell containing 500 ml of various electrolyte of NaCl and H_2SO_4 aqueous solutions at 25 °C. A platinum electrode used as the auxiliary electrode and calomel reference electrode used as the reference electrode while the steady state open circuit potential (OCP) noted. A new specimen used for each run. The potentiodynamic polarization study made from -500 mV versus OCP to +500 mV versus OCP at scan rate of 0.833 V/s, then measuring the corrosion currents. The corrosion current density (I_{corr}) and corrosion potential (E_{corr}) determined from Tafel plots of potential versus logarithm of corrosion current density. The corrosion rate (CR) calculated as follows in Eq. 2 [19-22]:

$$\text{CR (mm/yr)} = (0.00327 \times I_{\text{corr}} \times \text{eq.Wt})/D \quad (2)$$

Where I_{corr} is current density in $\mu\text{A/cm}^2$, D is the density in g/cm^3 ; eq.wt is the equivalent weight in grams.

2.3 Cyclic Voltammetry

Cyclic voltammetry is a powerful and popular electro-chemical technique which commonly apply for studying the chemical reactions of molecular species and invaluable. Also, to investigate electron transfer-initiated chemical reactions, including catalysis. Cyclic voltammetry studies were made from -1200 mv to 200 mv at three different scan rates of 20, 50, and 100 V/s [23-25].

2.4 Surface morphology

Morphology and analysis of corroded 304 SS were performed using SEM, EDX and mapping for elemental distribution.

3. RESULTS AND DISCUSSION

3.1. Weight loss

Figs. 1 and 2 show the relation between weight-loss and corrosion rate of 304 SS against exposure time in different concentrations of acidic media, respectively.

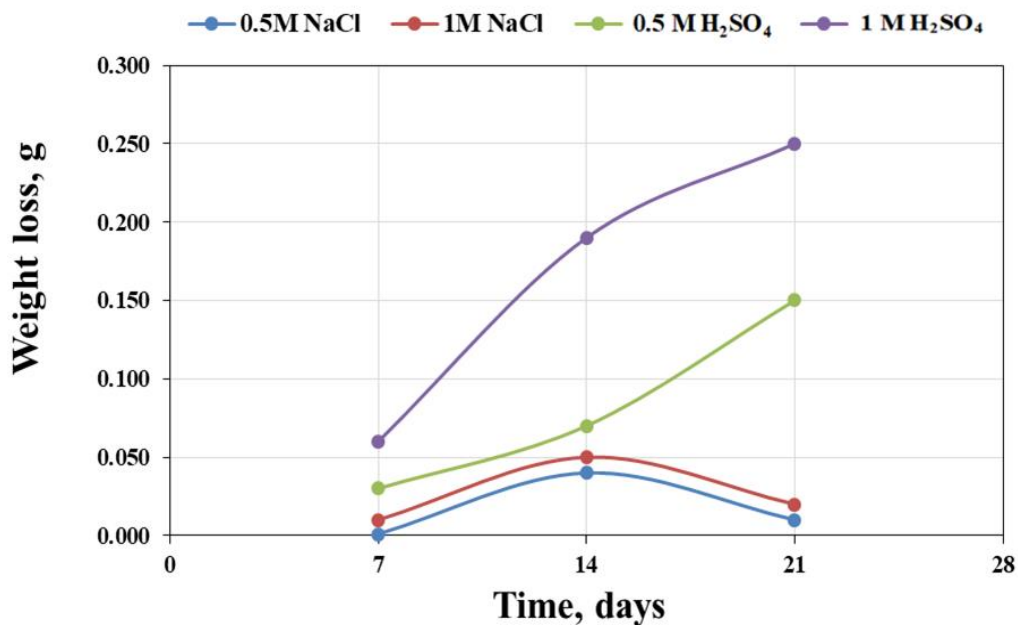


Figure 1. Weight-loss against exposure time for 304 SS immersed in different concentrations of acidic solution at 25 °C

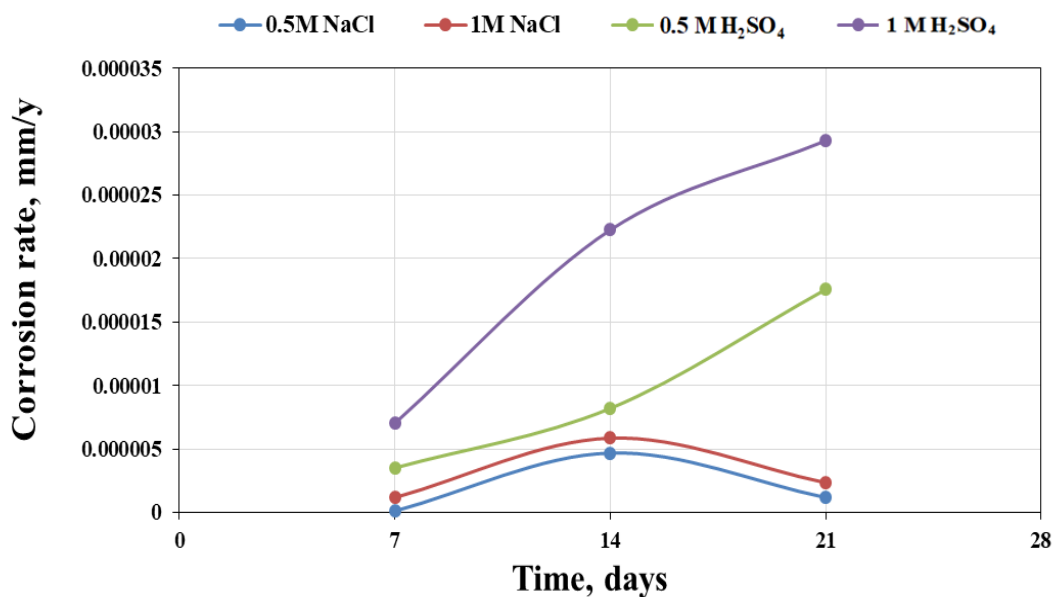


Figure 2. Corrosion rate against exposure time for 304 SS immersed in different concentrations of acidic solution in 25 °C

The weight-loss slightly decreased and corrosion rate increased with increase in the exposure time of NaCl solution. On the other hand, with addition of H₂SO₄, weight-loss sharply decreased and corrosion rate increased as exposure time increased.

3.2. Potentiodynamic Polarization

Fig. 3 provides the variation of potential E with logarithmic of the current density for 304 SS in the dilute NaCl and H₂SO₄ in different concentrations. Table 1 lists the electrochemical data at scan rate 0.833 V/s.

Table 1. The electrochemical data at scan rate 0.833 V/s

| Solution | E _{corr} , mV | i _{corr} , μA/cm ² | R _p , ohm.cm ² | CR, mm/yr |
|--------------------------------------|------------------------|--|--------------------------------------|-----------|
| 0.5 M H ₂ SO ₄ | -375 | 0.339 | 0.058 | 2.314 |
| 1 M H ₂ SO ₄ | -392 | 2.596 | 0.007 | 17.740 |
| 0.5 M NaCl | -312 | 5.129 | 6.620 | 0.035 |
| 1M NaCl | -286 | 3.037 | 7.440 | 0.021 |

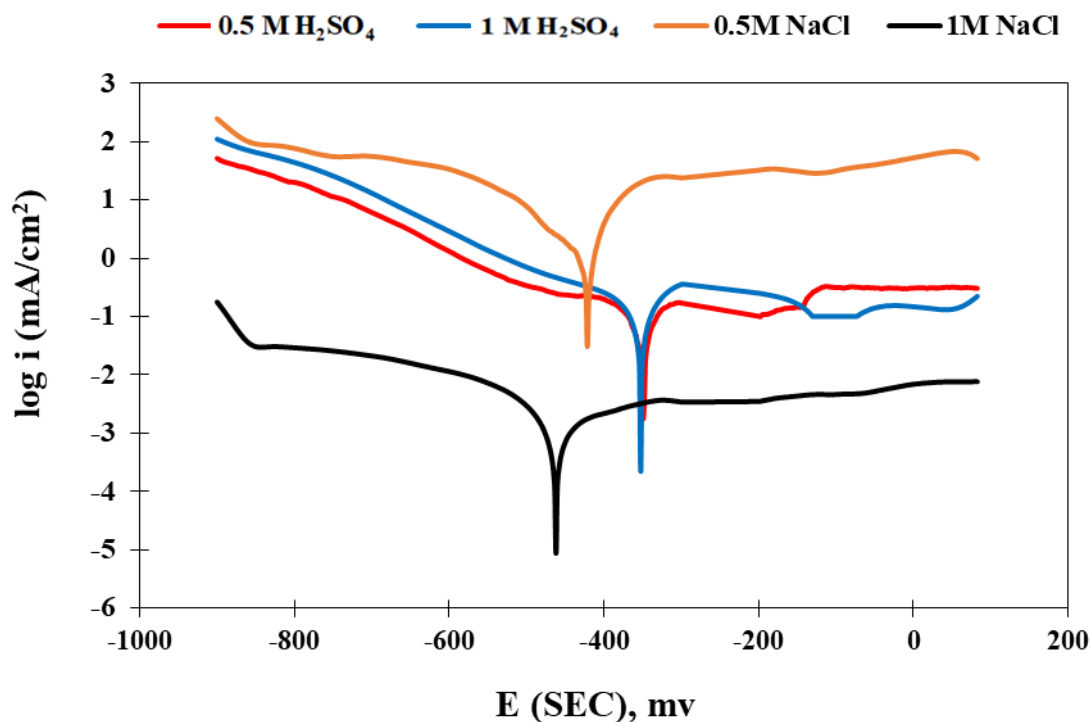


Figure 3. Polarization curves for 304 SS in different concentrations of NaCl and H₂SO₄ at scan rate 0.833 V/s at 25 °C

The 304 SS show the highest corrosion resistance in the 1M NaCl. Although the 304 SS show higher corrosion rate in 1M H₂SO₄ than 0.5 M H₂SO₄, but has the long area of pitting passivation rather than in 0.5M H₂SO₄ [19]. Increasing NaCl concentration shifts the corrosion potential of 304 SS to negative potential which is corresponding to decreasing the corrosion rate. On the other hand increasing the H₂SO₄ concentration shifts the corrosion potential of 304 SS to positive potential, so that the corrosion rate increased. The H₂SO₄ is more aggressive than NaCl due to its acidity.

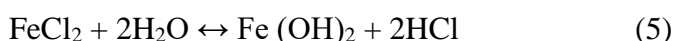
The existence of some alloying elements, such as Cr, is a very important factor for stabilizing the alloy behavior against general corrosion and localized corrosion. Playing a role for Fe and Ni-base metals. It accumulates in the passive layer because of its extremely small dissolution currents even in strongly acidic electrolytes. During corrosion, the anodic reaction inside the pit occurs according to the following reaction:



Electrons by the anode flow to the cathode (passivated surface), whereas they are discharged in the following cathodic reaction:

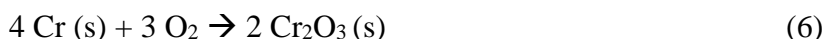


As a result of these reactions; the electrolyte inside the pit gains positive electrical charge in contrast to the electrolyte surrounding the pit, which becomes negatively charged. The positively charged pit attracts negative ions of chlorine for increasing acidity of the electrolyte according to the following reaction:



Greater corrosion rate formed due to the aggressive nature of the ionic species.

In addition, chromium oxides in aqueous solutions to produce Cr₂O₃ as in the following reaction:



These oxides and hydroxides precipitate on the metal surface led to transfer of metal from an active state to a passive state [26].

The 304 SS was aggressive attached with Cl⁻ ions and initiate pitting because of small size of Cl⁻ ions which enables penetration through the passive oxide film under electric field effect. The electric field enhanced to maintain electrical neutrality and hydrolysis of the corrosion products inside pits and causing acidification and hence preventing repassivation when it migration. This mechanism is autocatalytic due to acidity accelerates increasing of the dissolution rate inside pits. The effects of Cl⁻ ion concentration on polarization curves as well as on the Tafel lines of 304 SS in different concentrations of H₂SO₄ is given in Table (1). The electrochemical parameters values such as I_{corr}, E_{corr}, and corrosion rate at different concentrations of the NaCl and H₂SO₄. For all studied samples, the value

of I_{corr} increases with increasing of H_2SO_4 concentration. In case of increasing NaCl concentration, the 304 SS electrode is passive due to the Fe and Cr oxides formation.

3.3. Cyclic Voltammetry

The scan rate effect on the shape of the voltammetric profiles of 304 SS specimens immersed in either NaCl concentrations or H_2SO_4 concentrations was investigated in the 20 to 100 mV s^{-1} range. Figs. 4, 5, 6 and 7 give cyclic voltammetry curves in the two solutions. In the case of the specimen immersed in 0.5 and 1 M NaCl concentrations, and in the range of negative potentials, the oxidation and reduction peaks current increases with the increase of the potential scan rates. On the other hand, in the 0.5 and 1 M H_2SO_4 concentrations, the height of the current oxidation and reduction peaks increased as the potential sweep rate increased. In the small going sweep, a small current peak corresponding to the resistance of the 304 SS is observed. For H_2SO_4 and NaCl media, the cyclic voltammetry curves show that the current was exclusively faradaic contribution. Finally, the corrosion resistance of 304 SS is decreased in H_2SO_4 , but it increased in NaCl due to formation of passive layers of iron and chromium oxides. Similar results have been reported for 304 SS in methanolic solution of hydrochloric acid to which sulphuric acid was added [7, 23]

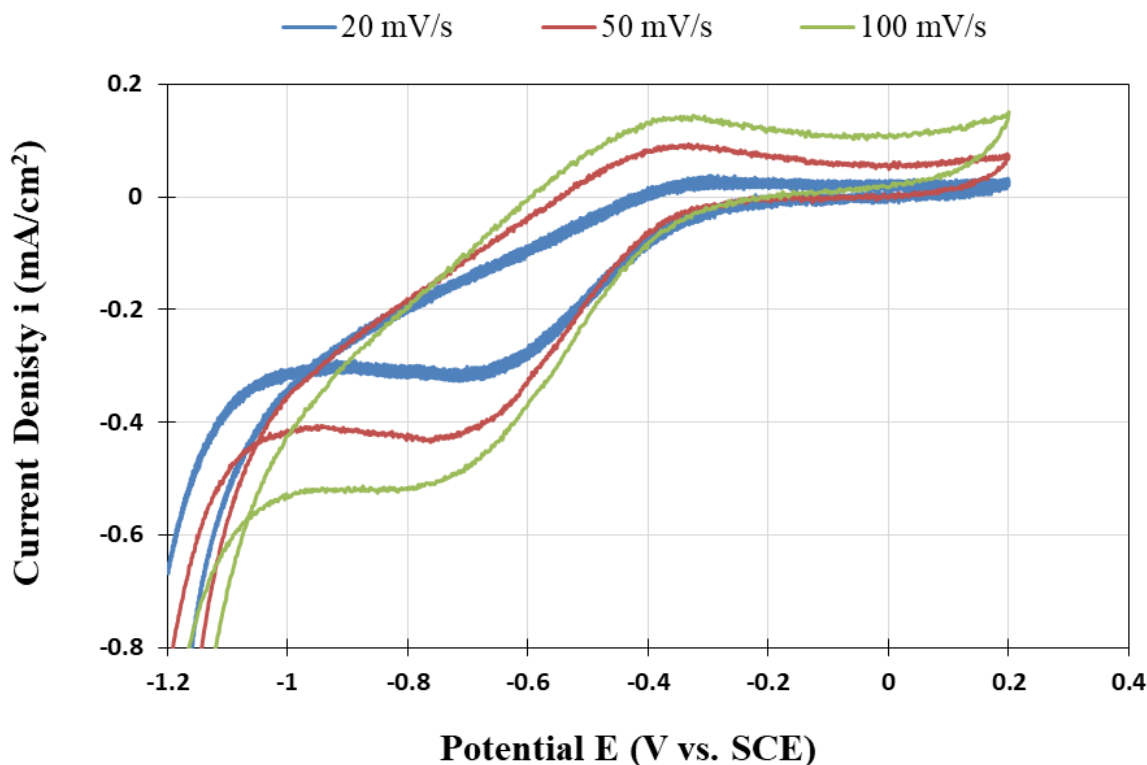


Figure 4. Cyclic voltammetry curves of 304 SS in 0.5 M NaCl at different scan rates at 25 °C

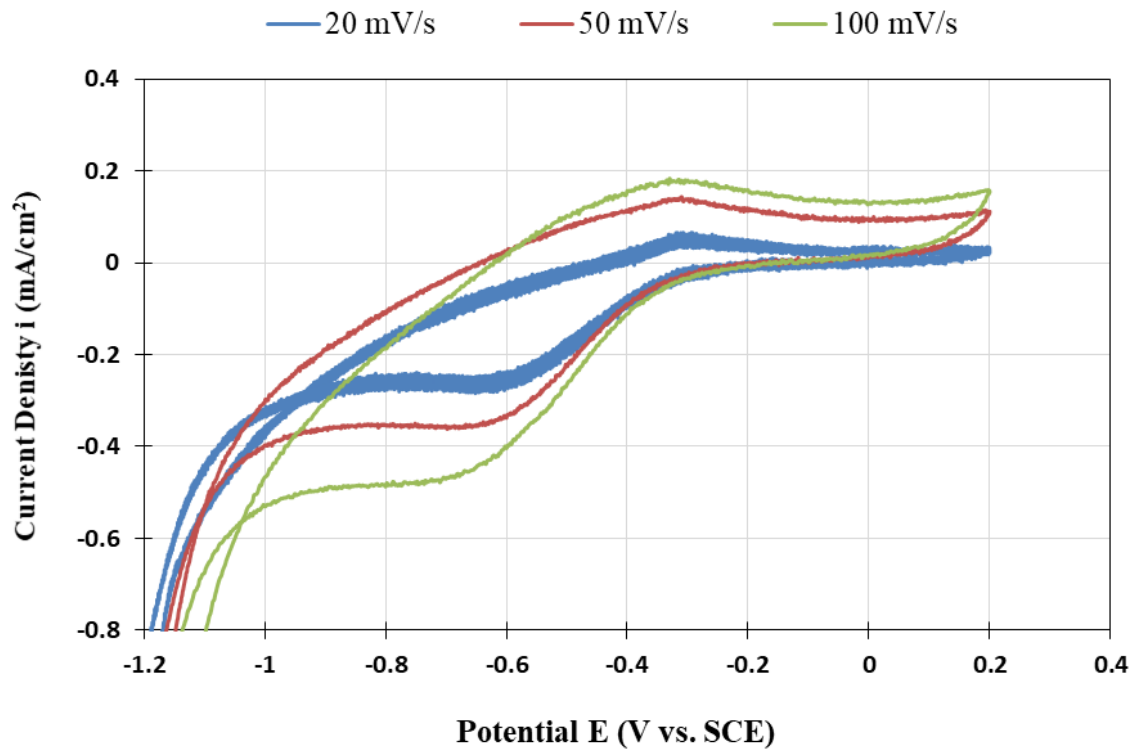


Figure 5. Cyclic voltammetry curves of 304 SS in 1 M NaCl at different scan rates at 25 °C

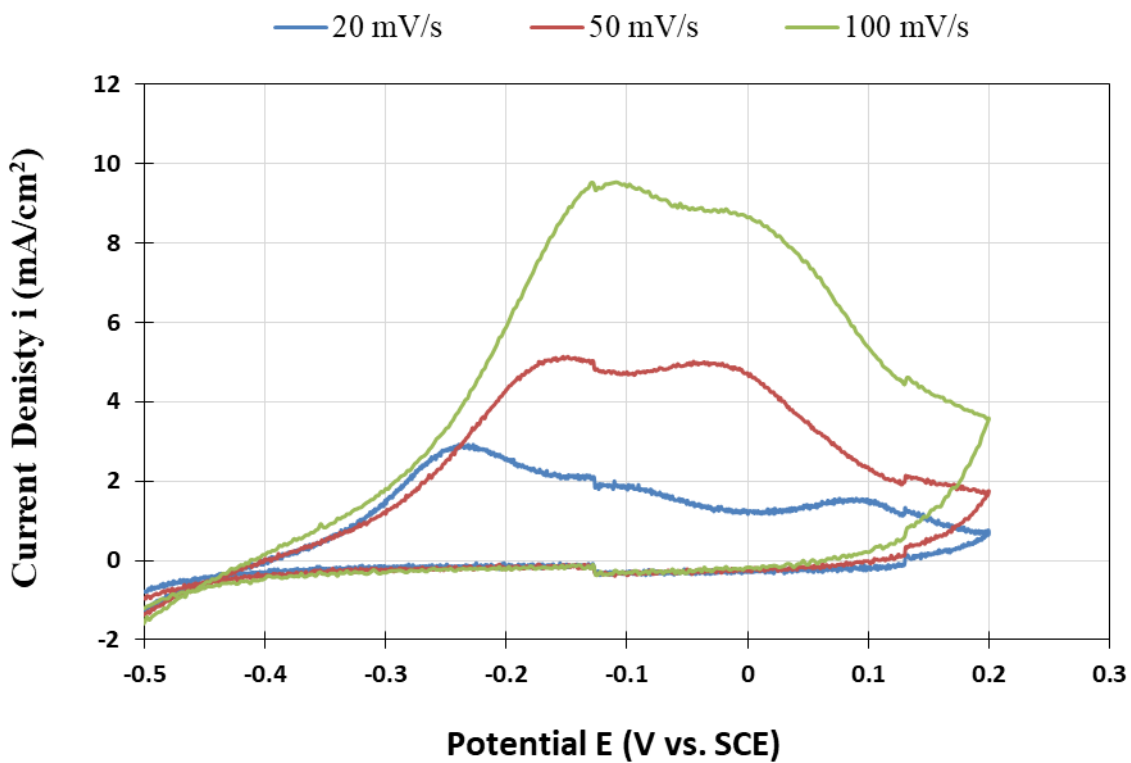


Figure 6. Cyclic voltammetry curves of 304 SS in 0.5 M H₂SO₄ at different scan rates at 25 °C

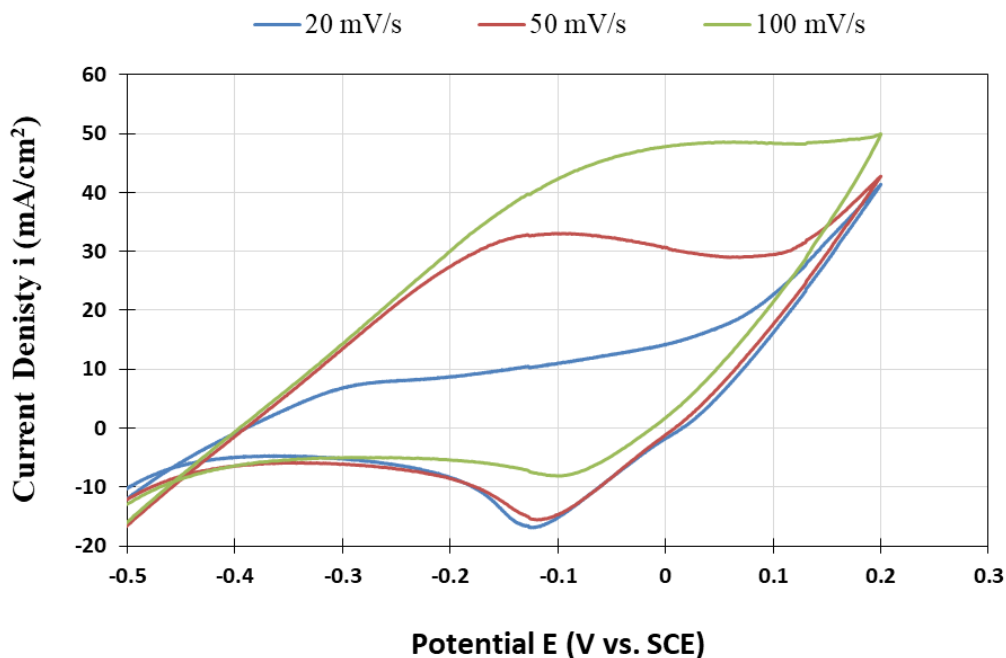


Figure 7. Cyclic voltammetry curves of 304 SS in 1 M H₂SO₄ at different scan rates at 25 °C

3.4 Microstructure of 304 SS

The SEM micrographs, EDX patterns, and mapping of 304 SS immersed in different concentrations are shown in Figs. 8, 9 and 10, respectively. Table 2 represents the EDX results of the different concentrations of NaCl. From the surface morphologies, pitting corrosion and general corrosion are existed in different concentrations of NaCl. Small pits are present in the passive layer then pits penetration increases with chloride-ion concentration increasing. Accelerated pitting corrosion causes hill and valley topology on 304 SS surface.

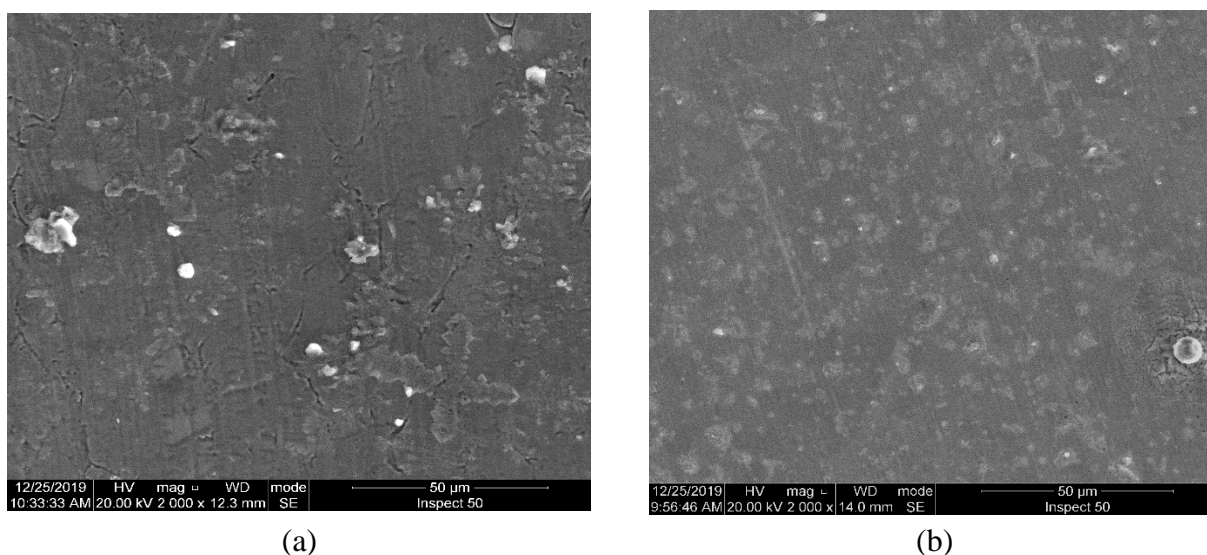


Figure 8. SEM images of 304 SS in (a) 0.5 M NaCl and (b) 1 M NaCl

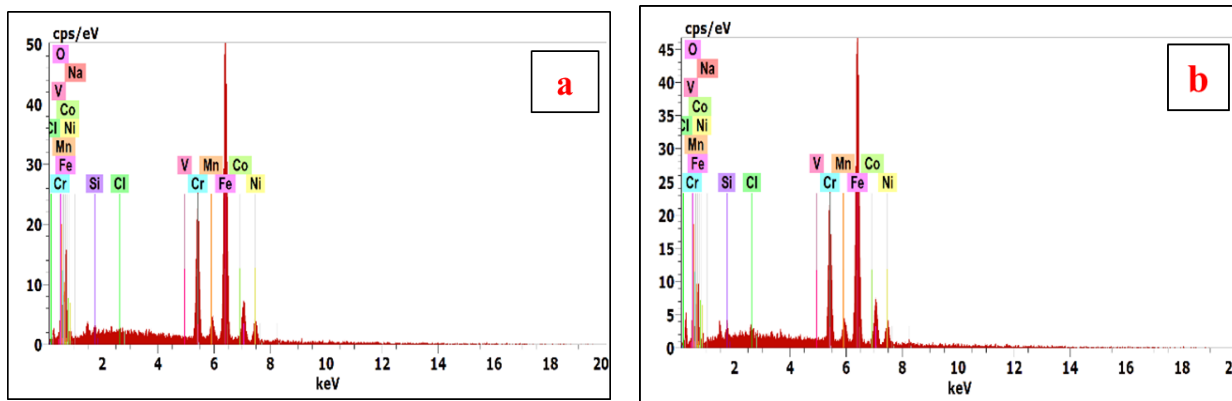
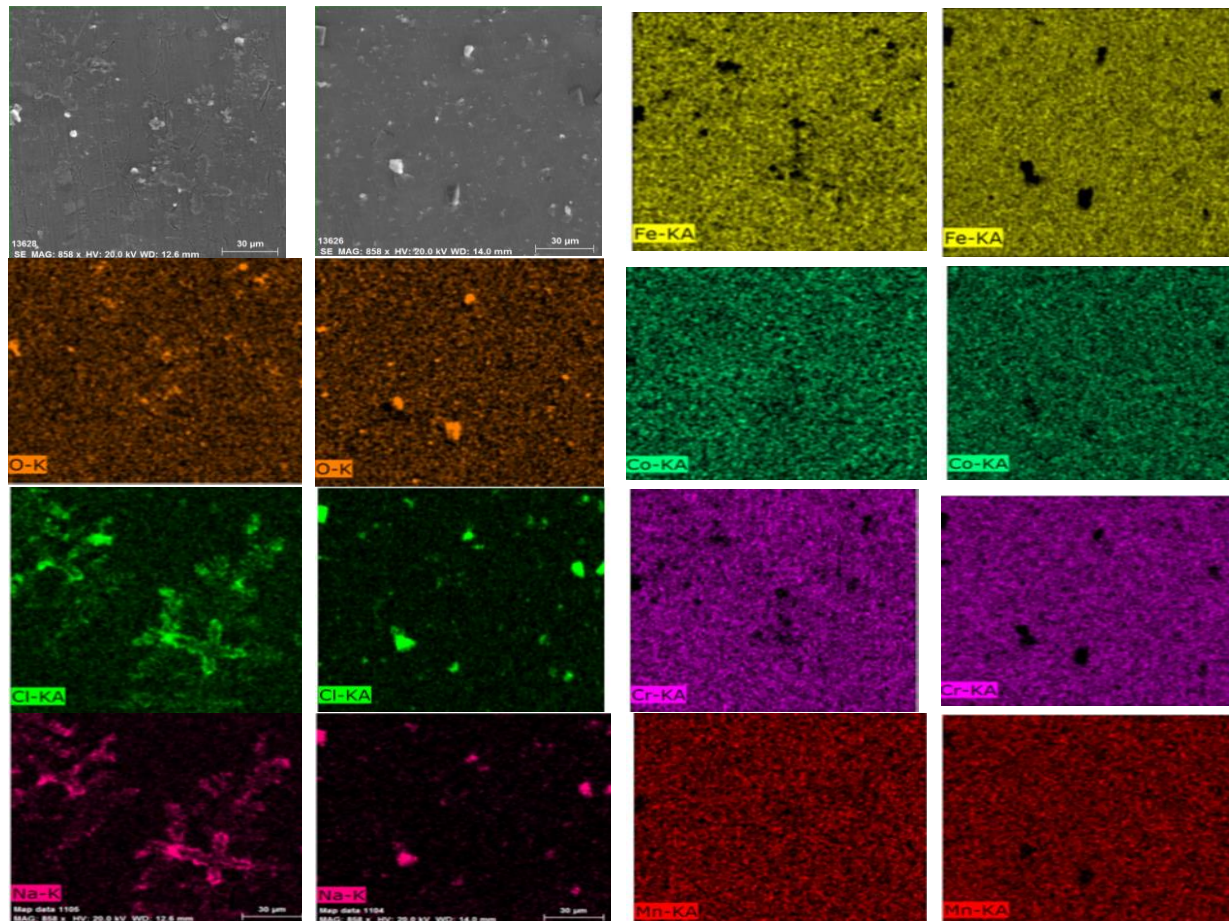


Figure 9. EDX analysis of 304 SS in (a) 0.5 M NaCl and (b) 1 M NaCl

Table 2. EDX analysis of corroded 304 SS in different concentrations of NaCl in wt.%

| Concentration NaCl | Elements in wt.% | | | | | | | | | |
|--------------------|------------------|------|------|------|------|------|-------|------|------|------|
| | O | Na | Cl | V | Si | Co | Cr | Mn | Ni | Fe |
| 0.5 M | 0.52 | 0.15 | 0.11 | 0.17 | 0.33 | 0.60 | 18.9 | 0.93 | 7.29 | Bal. |
| 1.0 M | 3.59 | 1.57 | 0.45 | 0.03 | 1.15 | 0.41 | 17.14 | 0.91 | 6.78 | Bal. |



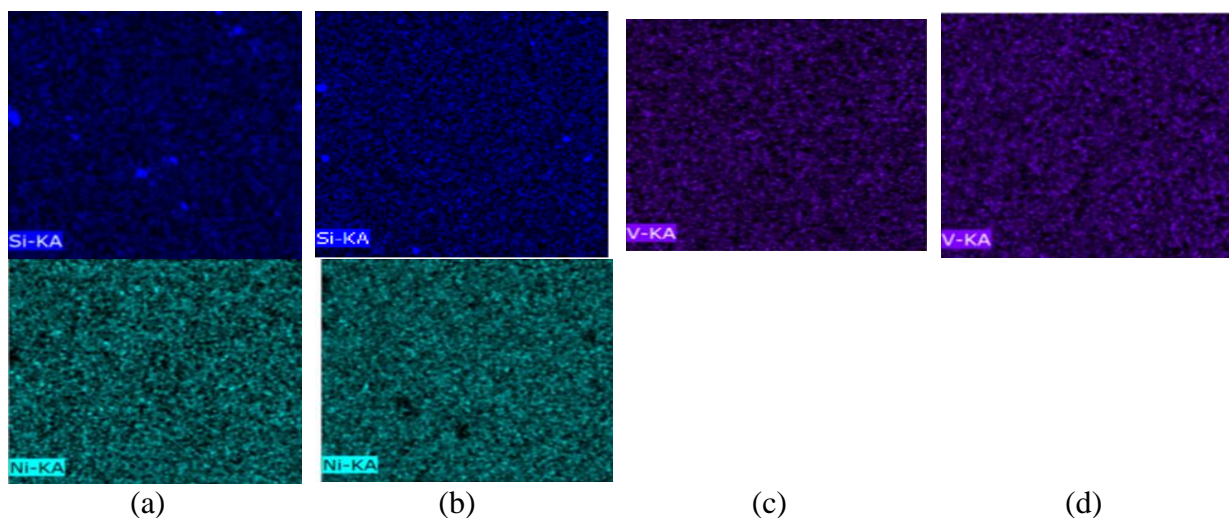


Figure 10. SEM images for 304 SS in NaCl (a, c) 0.5M NaCl and (b, d) 1 M NaCl

The SEM micrographs, EDX patterns, and mapping made for 304 SS immersed in different concentrations are shown in Figs. 11, 12 and 13, respectively. Table 3 represents the EDX results of the different concentrations of H₂SO₄ acid. In both acid concentrations, the corrosion reaction species are sulphate ions (SO⁴⁻) which breakdown the Cr₂O₃ passive film on 304 SS achieved by penetrating through the passive film to begin the corrosion reactions at its surface. The corrosion damage in the micrographs was noticed due to the effect of sulphate ions (SO₄) in 1M H₂SO₄ acid solution which accelerated the breakdown of the chromium film similar to those earlier discussed. The obtained EDX pattern indicate the existence of S in the passive film which may be rupture the oxide film while simultaneously initiating pitting. Fig. 13 illustrates the agglomeration of sulfides in some regions. There are a pitting corrosion in 304 SS surface which immersed in 1M H₂SO₄ [27]

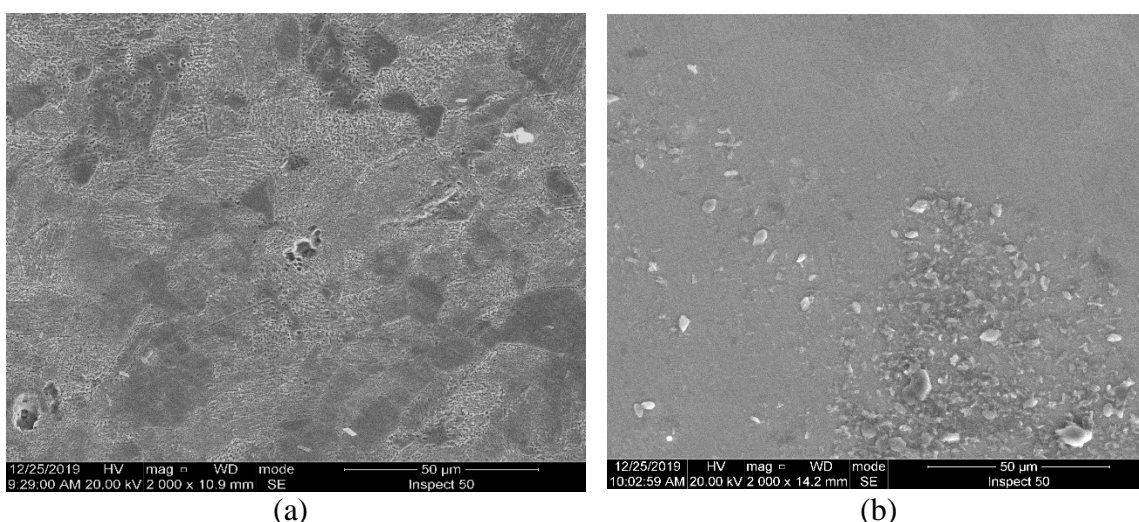


Figure 11. The SEM images of 304 SS in (a) 0.5 M H₂SO₄ and (b) 1 M H₂SO₄

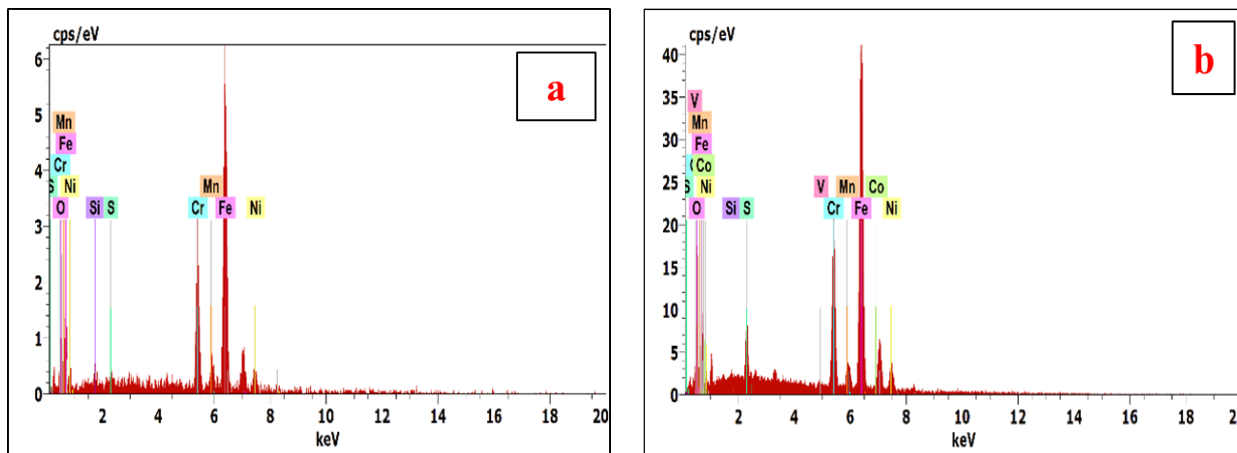
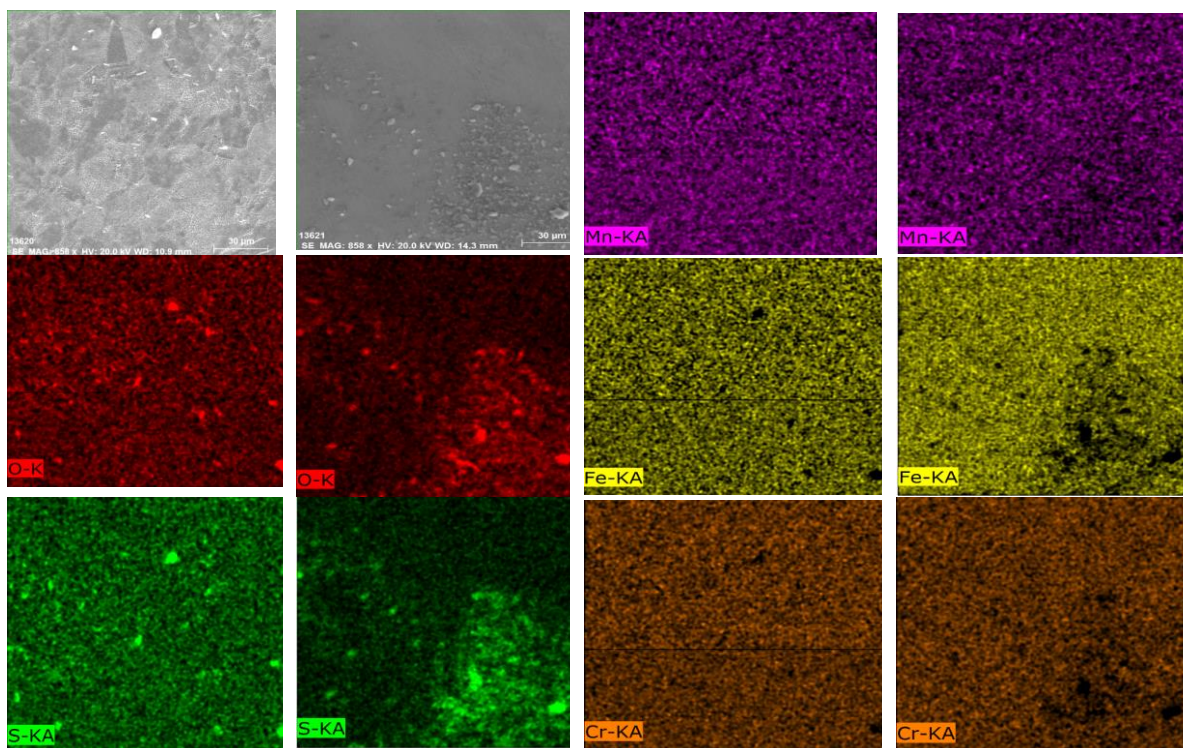


Figure 12. EDX analysis of 304 SS in H₂SO₄ (a) 0.5 M and (b) 1 M

Table 3. EDX analysis of corroded 304 SS in different concentrations of H₂SO₄ in wt.%

| Concentration H ₂ SO ₄ | Elements in wt.% | | | | | | | | |
|--|------------------|------|------|------|------|-------|------|------|------|
| | O | S | V | Si | Co | Cr | Mn | Ni | Fe |
| 0.5 M | 1.7 | 0.12 | 0 | 0.51 | 0 | 18.79 | 1.58 | 6.23 | Bal. |
| 1.0 M | 10.0 | 2.41 | 0.14 | 0.21 | 1.19 | 14.36 | 0.79 | 7.82 | Bal. |



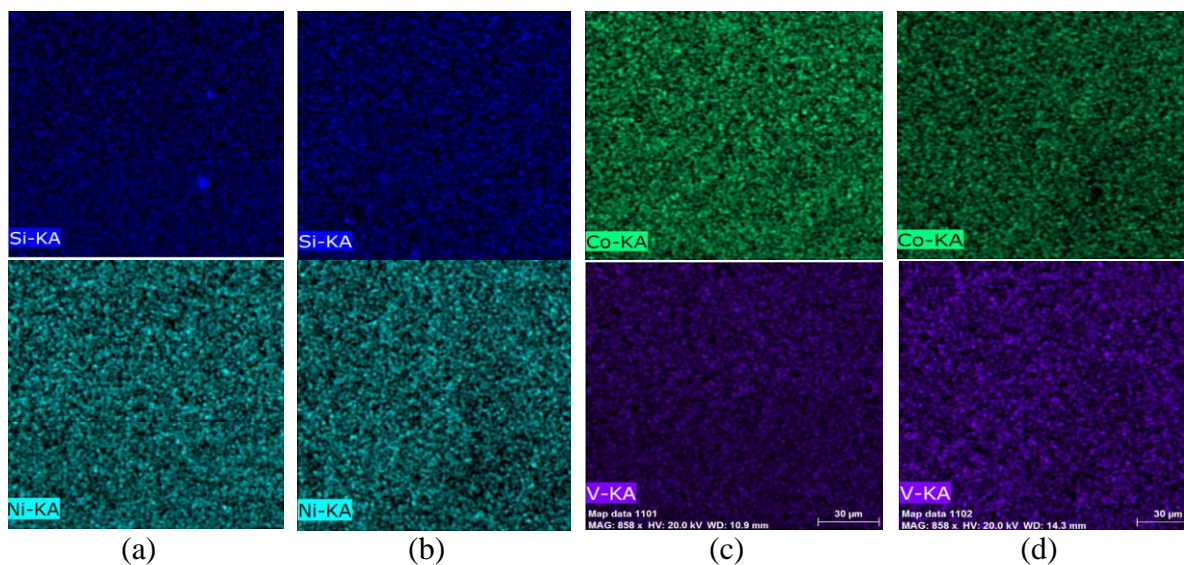


Figure 13. SEM images for 304 SS in H₂SO₄ (a, c) 0.5M and (b, d) 1 M

4. CONCLUSIONS

Pitting corrosion resistance of 304 SS investigated in 0.5M and 1.0M concentrations of both NaCl and H₂SO₄ solutions. Corrosion rates studied by chemical and electrochemical methods. Also, cyclic voltammetry curves investigated with different scan rates for different conditions in the investigated media. The surface morphology of corroded 304 SS examined by SEM, EDX and mapping. The weight-loss and corrosion rate of 304 SS in H₂SO₄ are higher than in NaCl. The polarization curves of 0.5M and 1M NaCl demonstrate that the higher the molarity of NaCl, the larger potential at which pitting occurs. Higher corrosion resistance of 304 SS in 1 M NaCl than other concentrations was confirmed by weight-loss, polarization and cyclic voltammetry. At lower concentrations, results show that, a decrease in the passive regions in the H₂SO₄ as compared to the NaCl, due to destruction of Cr₂O₃ passive film. This destruction is formed due to high diffusivity of the chloride and sulfide ions through cracks which breakdown faster than the repassivation rate. This forms pits by autocatalytic mechanism. Increasing NaCl concentration led to only delays the pits formation but still enhances the corrosion behavior. Surface morphologies of corroded 304SS in different concentrations of H₂SO₄ have a significant pitting corrosion and extensive damage of the passive layer than in NaCl solution.

ACKNOWLEDGEMENT

The authors acknowledge Associate Prof. Yassar Reda (Higher Institute of Engineering and Technology Tanta) for English revision

References

1. K.V.S. Ramana, T. Anita, S. Mandal, S. Kaliappan, H. Shaikh, P.V. Sivaprasad, R.K. Dayal, H.S. Khatak, *Mater Des.*, 30 (2009) 3770–3775

2. A. Fouda, H. El-Abbasy, *Corros. J Sci Eng.*, 68 (2012) 015002–1-015002-9
3. V. Alar, I. Žmak, B. Runje, A. Horvatić, *Int. J. Electrochem. Sci.*, 11 (2016) 7674–7689
4. A. Pardo, M. Merino, A. Coy, F. Viejo, R. Arrabal, E. Matykina, *Corros Sci.*, 50 (2008) 1796–1806
5. J. Polo, E. Cano, J. Bastidas, *J Electroanal Chem.*, 537 (2002) 183–187
6. S. Hastuty, A. Nishikata, T. Tsuru, *Corros. Sci.*, 52 (2010) 2035–2043
7. E. Bardal, Corrosion and Protection, *Springer Science and Business Media*, (2007)
8. Y. Sun, J. Wang, Y. Jiang, J. Li, *Mater Corros.*, 69 (2018) 44–52
9. S.M. Lee, W.G. Lee, Y.H. Kim, H. Jang, *Corros Sci.*, 63 (2012) 404–409
10. A. Pachón-Montaño, J. Sánchez-Montero, C. Andrade, J. Fulla, E. Moreno, V. Matres, *Constr Build Mater.*, 186 (2018) 495–502
11. M.A. Ibrahim, S.A. El Rehim, M. Hamza, *Mater Chem Phys.*, 115 (2009) 80–85
12. M. Shabani-Nooshabadi, M. Ghandchi, *J Ind Eng Chem.*, 31 (2015) 231–237
13. H.H. Strehblow, Corrosion Mechanisms in Theory and Practice, New York, (2002) 349–390
14. R.T. Loto, *J Mater Environ Sci.*, 6 (10) (2015) 2750-2762
15. R. Ke, R. Alkire, *J Electrochem Soc.*, 142(12) (1995) 4056–4062
16. D.D. Macdonald, D.F. Heaney, *Corros Sci.*, 42(10) (2000) 1779–1799
17. D.E. Williams, T.F. Mohiuddin, Y.Y. Zhu, *J Electrochem Soc.*, 145(8) (1998) 2664–2672
18. A.A. Dastgerdi, A. Brenna, M. Ormellese, M. Pedeferrri, F. Bolzoni, *Corros Sci.*, 159 (2019) 108160
19. C.A. Loto, O.S.I. Fayomi, R.T. Loto, A.P.I. Popool, *Procedia Manufacturing*, 35 (2019) 413–418
20. SR. Al-Sayed, A. Abdelfatah, *Metallogr Microstruct Anal.*, 9 (2020) 553–560
21. A. Abdelfatah, M. Abu-Okail, L.Z. Mohamed, *Int J Electrochem Sci.*, 16 (2021) 151001
22. L.Z. Mohamed, M.A.H. Gepreel, A. Abdelfatah, *Chem Papers*, 75(12), (2021) 6265-6274
23. Y. Ait Albrimi, A. Eddib, J. Douch, Y. Berghoute, M. Hamdani, R.M. Souto, *Int J Electrochem Sci.*, 6 (2011) 4614 -4627
24. N. Elgrishi, K.J. Rountree, B.D. McCarthy, E.S. Rountree, T.T. Eisenhart, J.L. Dempsey, *J Chem Educ.*, (2018) 197–206
25. M. Pandiarajan, S. Rajendran, J.S. Bama, *Int J Nano Corr Sci Eng.*, 3(4) (2016)166–180
26. D.H. Abdeen, M.A. Atieh, B. Merzougui, W. Khalfaoui, *Materials*, 12 (2019) 1634
27. G.A. Gaber, S. Hosny, L.Z. Mohamed, *Int J Electrochem Sci.*, 16 (2021) 211214